Measurements of Branching Fractions for $B \to K\pi$ and $B \to \pi\pi$ Decays with 449 million $B\overline{B}$ Pairs

S.-W. Lin,[25] P. Chang,[25] K. Abe,[9] K. Abe,[43] I. Adachi,[9] H. Aihara,[45] D. Anipko,[1] V. Aulchenko,[1] T. Aushev,[17,13] S. Bahinipati,[3] A. M. Bakich,[41] E. Barberio,[20] I. Bedny,[1] U. Bitenc,[14] I. Bizjak,[14] S. Blyth,[23] A. Bondar,[1] A. Bozek,[26] M. Bračko,[9,19,14] T. E. Browder,[8] M.-C. Chang,[4] Y. Chao,[25] A. Chen,[23] K.-F. Chen,[25] W. T. Chen,[23] B. G. Cheon,[7] R. Chistov,[13] S.-K. Choi,[6] Y. Choi,[40] Y. K. Choi,[40] J. Dalseno,[20] M. Dash,[49] J. Dragic,[9] A. Drutskoy,[3] S. Eidelman,[1] S. Fratina,[14] N. Gabyshev,[1] A. Garmash,[34] A. Go,[23] B. Golob,[18,14] H. Ha,[16] J. Haba,[9] T. Hara,[31] H. Hayashii,[22] M. Hazumi,[9] D. Heffernan,[31] T. Hokuue,[21] Y. Hoshi,[43] W.-S. Hou,[25] Y. B. Hsiung,[25] T. Iijima,[21] K. Ikado,[21] A. Imoto,[22] K. Inami,[21] A. Ishikawa,[45] H. Ishino,[46] R. Itoh,[9] M. Iwasaki,[45] Y. Iwasaki,[9] H. Kaji,[21] P. Kapusta,[26] S. U. Kataoka,[22] H. Kawai,[2] T. Kawasaki,[28] H. Kichimi,[9] Y. J. Kim,[5] K. Kinoshita,[3] S. Korpar,[19,14] P. Križan,[18,14] P. Krokovny,[9] R. Kulasiri,[3] R. Kumar,[32] A. Kuzmin,[1] Y.-J. Kwon,[50] M. J. Lee,[38] T. Lesiak,[26] D. Liventsev,[13] J. MacNaughton,[11] F. Mandl,[11] T. Matsumoto,[47] S. McOnie,[41] T. Medvedeva,[13] W. Mitaroff,[11] H. Miyake,[31] H. Miyata,[28] Y. Miyazaki,[21] G. R. Moloney,[51] E. Nakano,[30] M. Nakao,[9] H. Nakazawa,[23] Z. Natkaniec,[26] S. Nishida,[9] O. Nitoh,[48] S. Ogawa,[42] T. Ohshima,[21] S. Okuno,[15] S. L. Olsen,[8] Y. Onuki,[35] H. Ozaki,[9] P. Pakhlov,[13] G. Pakhlova,[13] C. W. Park,[40] R. Pestotnik,[14] L. E. Piilonen,[49] H. Sahoo,[8] Y. Sakai,[9] N. Satoyama,[39] T. Schietinger,[17] O. Schneider,[17] J. Schümann,[9] A. J. Schwartz,[3] K. Senyo,[21] M. E. Sevior,[20] M. Shapkin,[12] H. Shibuya,[42] B. Shwartz,[1] J. B. Singh,[32] A. Somov,[3] N. Soni,[32] S. Stanič,[29] M. Starič,[14] H. Stoeck,[41] K. Sumisawa,[9] T. Sumiyoshi,[47] S. Suzuki,[36] S. Y. Suzuki,[9] F. Takasaki,[9] K. Tamai,[9] M. Tanaka,[9] G. N. Taylor,[20] Y. Teramoto,[30] X. C. Tian,[33] I. Tikhomirov,[13] T. Tsukamoto,[9] S. Uehara,[9] K. Ueno,[25] Y. Unno,[7] S. Uno,[9] Y. Ushiroda,[9] G. Varner,[8] K. E. Varvell,[41] S. Villa,[17] C. C. Wang,[25] C. H. Wang,[24] M.-Z. Wang,[25] Y. Watanabe,[46] J. Wicht,[17] E. Won,[16] Q. L. Xie,[10] B. D. Yabsley,[41] A. Yamaguchi,[44] Y. Yamashita,[27] M. Yamauchi,[9] Y. Yusa,[49] C. C. Zhang,[10] Z. P. Zhang,[37] and A. Zupanc[14]

(The Belle Collaboration)

[1] *Budker Institute of Nuclear Physics, Novosibirsk*
[2] *Chiba University, Chiba*
[3] *University of Cincinnati, Cincinnati, Ohio 45221*
[4] *Department of Physics, Fu Jen Catholic University, Taipei*
[5] *The Graduate University for Advanced Studies, Hayama*
[6] *Gyeongsang National University, Chinju*
[7] *Hanyang University, Seoul*
[8] *University of Hawaii, Honolulu, Hawaii 96822*
[9] *High Energy Accelerator Research Organization (KEK), Tsukuba*
[10] *Institute of High Energy Physics, Chinese Academy of Sciences, Beijing*
[11] *Institute of High Energy Physics, Vienna*
[12] *Institute of High Energy Physics, Protvino*
[13] *Institute for Theoretical and Experimental Physics, Moscow*
[14] *J. Stefan Institute, Ljubljana*
[15] *Kanagawa University, Yokohama*
[16] *Korea University, Seoul*
[17] *Swiss Federal Institute of Technology of Lausanne, EPFL, Lausanne*
[18] *University of Ljubljana, Ljubljana*
[19] *University of Maribor, Maribor*
[20] *University of Melbourne, Victoria*
[21] *Nagoya University, Nagoya*
[22] *Nara Women's University, Nara*
[23] *National Central University, Chung-li*
[24] *National United University, Miao Li*
[25] *Department of Physics, National Taiwan University, Taipei*
[26] *H. Niewodniczanski Institute of Nuclear Physics, Krakow*
[27] *Nippon Dental University, Niigata*
[28] *Niigata University, Niigata*
[29] *University of Nova Gorica, Nova Gorica*
[30] *Osaka City University, Osaka*
[31] *Osaka University, Osaka*

[32]Panjab University, Chandigarh
[33]Peking University, Beijing
[34]Princeton University, Princeton, New Jersey 08544
[35]RIKEN BNL Research Center, Upton, New York 11973
[36]Saga University, Saga
[37]University of Science and Technology of China, Hefei
[38]Seoul National University, Seoul
[39]Shinshu University, Nagano
[40]Sungkyunkwan University, Suwon
[41]University of Sydney, Sydney, New South Wales
[42]Toho University, Funabashi
[43]Tohoku Gakuin University, Tagajo
[44]Tohoku University, Sendai
[45]Department of Physics, University of Tokyo, Tokyo
[46]Tokyo Institute of Technology, Tokyo
[47]Tokyo Metropolitan University, Tokyo
[48]Tokyo University of Agriculture and Technology, Tokyo
[49]Virginia Polytechnic Institute and State University, Blacksburg, Virginia 24061
[50]Yonsei University, Seoul
[51]University of Melbourne, School of Physics, Victoria 3010

We report measurements of branching fractions for $B \to K\pi$ and $B \to \pi\pi$ decays based on a data sample of 449 million $B\overline{B}$ pairs collected at the $\Upsilon(4S)$ resonance with the Belle detector at the KEKB asymmetric-energy e^+e^- collider. We also calculate the ratios of partial widths for the decays $B \to K\pi$, namely $R_c = 1.08 \pm 0.06 \pm 0.08$ and $R_n = 1.08 \pm 0.08^{+0.09}_{-0.08}$,where the first and the second errors are statistical and systematic, respectively. These ratios are sensitive to enhanced electroweak penguin contributions from new physics; the new measurements are, however, consistent with Standard Model expectations.

PACS numbers: 11.30.Er, 12.15.Hh, 13.25.Hw, 14.40.Nd

Tests of the Standard Model (SM) can be performed in B-meson decays to $K\pi$ and $\pi\pi$ final states, which involve various interplays between dominant $b \to u$ tree diagram, $b \to s$, d penguin diagrams and other sub-dominant contributions. In general, direct comparisons of the measured branching fractions with the SM predictions suffer from large hadronic uncertainties within the current theoretical framework. However, many of the uncertainties cancel out in ratios of branching fractions. Previous experimental results [1, 2, 3] for the ratios $R_c \equiv 2\Gamma(B^+ \to K^+\pi^0)/\Gamma(B^+ \to K^0\pi^+) = 1.00 \pm 0.08$ and $R_n \equiv \Gamma(B^0 \to K^+\pi^-)/2\Gamma(B^0 \to K^0\pi^0) = 0.82 \pm 0.08$ [4] deviate from the SM expectations within several approaches [5, 6, 7, 8]. For example, Ref. [5] predicts the values $R_c = 1.15 \pm 0.05$ and $R_n = 1.12 \pm 0.05$, which are calculated assuming $SU(3)$ flavor symmetry. If the differences between these SM expectations and the measured values of R_c and R_n persist with more data, this would imply a large electroweak penguin contribution in $B \to K\pi$ decays [5, 7, 8].

In this letter, we report new measurements of the branching fractions for $B \to K^+\pi^-$, $K^+\pi^0$, $K^0\pi^0$, $\pi^+\pi^-$ and $\pi^+\pi^0$ decays with a data sample five times larger than that used in our previous study [1]. Recent Belle results for $B \to K\overline{K}$, $B^+ \to K^0\pi^+$ and $B^0 \to \pi^0\pi^0$ decays have been reported elsewhere [9, 10]. The results are based on a sample of $(449.3 \pm 5.7) \times 10^6$ $B\overline{B}$ pairs collected with the Belle detector at the KEKB e^+e^- asymmetric-energy (3.5 on 8 GeV) collider [11]. The production rates of B^+B^- and $B^0\overline{B}^0$ pairs are assumed to be equal. The inclusion of the charge-conjugate decay is implied, unless explicitly stated otherwise.

The Belle detector is a large-solid-angle magnetic spectrometer that consists of a silicon vertex detector (SVD), a 50-layer central drift chamber (CDC), an array of aerogel threshold Cherenkov counters (ACC), a barrel-like arrangement of time-of-flight scintillation counters, and an electromagnetic calorimeter comprised of CsI(Tl) crystals located inside a superconducting solenoid coil that provides a 1.5 T magnetic field. An iron flux-return located outside the coil is instrumented to detect K^0_L mesons and to identify muons. The detector is described in detail elsewhere [12]. Two different inner detector configurations were used. For the first sample of 152 million $B\overline{B}$ pairs (set I), a 2.0 cm radius beampipe and a three-layer silicon vertex detector were used; for the latter 297 million $B\overline{B}$ pairs (set II), a 1.5 cm radius beampipe, a four-layer silicon detector and a small-cell inner drift chamber were used [13].

Primary charged tracks are required to have a distance of closest approach to the interaction point (IP) of less than 4 cm in the beam direction (z-axis) and less than 0.1 cm in the transverse plane. Charged kaons and pions are identified using dE/dx information from the CDC and Cherenkov light yields in the ACC, which are combined to form a K-π likelihood ratio $\mathcal{R}(K/\pi) = \mathcal{L}_K/(\mathcal{L}_K+\mathcal{L}_\pi)$,

where $\mathcal{L}_K$ ($\mathcal{L}_\pi$) is the likelihood that the track is a kaon (pion). Charged tracks with $\mathcal{R}(K/\pi) > 0.6$ (<0.4) are classified as kaons (pions). Typically, the kaon (pion) identification efficiency is 83% (90%), and 6% (12%) of selected kaons (pions) are misidentified as pions (kaons). Furthermore, we reject charged tracks that are consistent with an electron hypothesis. Candidate K^0 mesons are reconstructed as $K^0_S \to \pi^+\pi^-$ decays with the branching fraction taken from Ref. [14]. We pair oppositely-charged tracks assuming the pion hypothesis and require the invariant mass of the pair to be within ± 18 MeV/c^2 of the nominal K^0_S mass. The intersection point of the $\pi^+\pi^-$ pair must be displaced from the IP [15]. Pairs of photons with invariant masses in the range of 115 MeV/c^2 $< M_{\gamma\gamma} <$ 152 MeV/c^2 ($\pm 3\sigma$) are considered as π^0 candidates. The photon energy is required to be greater than 50 MeV in the barrel region, defined as $32^\circ < \theta_\gamma < 128^\circ$, and greater than 100 MeV in the end-cap regions, defined as $17^\circ < \theta_\gamma < 32^\circ$ or $128^\circ < \theta_\gamma < 150^\circ$, where θ_γ denotes the photon polar angle with respect to the direction anti-parallel to the e^+ beam.

Candidate B mesons are identified by the "beam-energy-constrained" mass, $M_{\rm bc} \equiv \sqrt{E^{*2}_{\rm beam}/c^4 - p^{*2}_B/c^2}$, and the energy difference, $\Delta E \equiv E^*_B - E^*_{\rm beam}$, where $E^*_{\rm beam}$ is the run-dependent beam energy, and E^*_B and p^*_B are the reconstructed energy and momentum of the B candidates in the center-of-mass (CM) frame, respectively. Events with $M_{\rm bc} > 5.20$ GeV/c^2 and $|\Delta E| <$ 0.3 GeV are selected for the analysis.

The dominant background is from $e^+e^- \to q\overline{q}$ ($q = u, d, s, c$) continuum events. We use event topology to distinguish the $B\overline{B}$ events from the jet-like continuum background. We combine a set of modified Fox-Wolfram moments [16] into a Fisher discriminant. A signal/background likelihood is formed, based on a GEANT-based [17] Monte Carlo (MC) simulation, from the product of the probability density functions (PDFs) for the Fisher discriminant and that for the cosine of the polar angle of the B-meson flight direction. Suppression of the continuum is achieved by applying a requirement on the ratio $\mathcal{R} = \mathcal{L}_{\rm sig}/(\mathcal{L}_{\rm sig}+\mathcal{L}_{q\overline{q}})$, where $\mathcal{L}_{\rm sig}$ ($\mathcal{L}_{q\overline{q}}$) is the signal (continuum) likelihood. Continuum background is further suppressed through use of the B-flavor tagging algorithm [18], which provides a discrete variable indicating the flavor of the tagging B meson and a continuous quality parameter r ranging from 0 (for no flavor-tagging information) to 1 (for unambiguous flavor assignment). Events with a high value of r are considered well-tagged and hence are unlikely to have originated from continuum processes. We classify events separately as poorly-tagged ($r \leq 0.5$) and well-tagged ($r > 0.5$) in data set I and data set II and for each category we determine a continuum suppression requirement for $\mathcal{R}$ that maximizes the value of $N^{\rm exp}_{\rm sig}/\sqrt{N^{\rm exp}_{\rm sig} + N^{\rm exp}_{q\overline{q}}}$. Here, $N^{\rm exp}_{\rm sig}$ denotes the expected signal yields based on MC simulation and the average branching fractions of the previous measurements [1, 2, 3], and $N^{\rm exp}_{q\overline{q}}$ denotes the expected continuum yields as estimated from sideband data ($M_{\rm bc} < 5.26$ GeV/c^2 and $|\Delta E| < 0.3$ GeV).

Background contributions from $\Upsilon(4S) \to B\overline{B}$ events are investigated using a large MC sample that includes events from $b \to c$ transitions and charmless B decays. After all the selection requirements, no $b \to c$ background is found, while a small contribution from charmless B decays is present at low ΔE values for all studied modes. Due to $K - \pi$ misidentification, large $B^0 \to K^+\pi^-$ and $B^+ \to K^+\pi^0$ feed-across backgrounds appear in the $B^0 \to \pi^+\pi^-$ and $B^+ \to \pi^+\pi^0$ modes, respectively.

The signal yields are extracted by performing extended unbinned maximum likelihood fits to the ($M_{\rm bc}$, ΔE) distributions of the selected candidate events. The likelihood function for each mode is defined as

$$\mathcal{L} = \frac{\exp\left(-\sum_{l,k,j} N_{l,k,j}\right)}{N!} \prod_i \left(\sum_{l,k,j} N_{l,k,j} P^i_{l,k,j}\right), \quad (1)$$

where N is the total number of events, i is the event identifier, l indicates set I or set II, k distinguishes the two r regions and j runs over all components included in the fitting function: signal, continuum background, feed-across, and charmless B background. The variable $N_{l,k,j}$ denotes the number of events, and $P^i_{l,k,j} = \mathcal{P}_{l,k,j}(M^i_{\rm bc}, \Delta E^i)$ are two-dimensional PDFs, which are the same in the two r regions for all fit components except for the continuum background.

All the signal PDFs ($P_{l,k,j={\rm signal}}(M_{\rm bc}, \Delta E)$) are parameterized by smoothed two-dimensional histograms obtained from correctly reconstructed signal MC based on the set I and set II detector configurations. Signal MC events are generated with the PHOTOS [19] simulation package to take into account final-state radiation. Since the $M_{\rm bc}$ signal distribution is dominated by the beam-energy spread, we use the signal-peak positions and resolutions obtained from $B^+ \to \overline{D}^0\pi^+$ data to refine our signal MC (the $\overline{D}^0 \to K^+\pi^-\pi^0$ sub-decay is used for modes with a π^0 in the final state, while $\overline{D}^0 \to K^+\pi^-$ is used for the other modes). The resolution for the ΔE distribution is calibrated using the invariant mass distribution of high momentum ($p_{\rm Lab} > 3$ GeV/c) D mesons. The size of the final-state radiation effects can be assessed if we take signal PDFs from MC without PHOTOS and use these PDFs to extract the signal yields from the signal MC with PHOTOS. The extracted yields decrease by 5.8% for $B^0 \to K^+\pi^-$, 9.4% for $B^0 \to \pi^+\pi^-$ and 3.6% for $B^+ \to K^+\pi^0$ and $B^+ \to \pi^+\pi^0$, respectively.

The continuum background PDF is described by a product of a linear function for ΔE and an ARGUS function, $f(x) = x\sqrt{1-x^2}\,\exp\left[-\xi(1-x^2)\right]$, where $x = M_{\rm bc}c^2/E^*_{\rm beam}$ [20]. The overall normalization, ΔE slope and ARGUS parameter ξ are free parameters in the fit. The background PDFs for charmless B decays are mod-

eled by a smoothed two-dimensional histogram, obtained from a large MC sample. We also use a smoothed two-dimensional histogram to describe the feed-across background, since the background events have ($M_{\rm bc}$, ΔE) shapes similar to the signal, except for a ΔE peak position shift of $\simeq 45$ MeV. We perform a simultaneous fit for $B^0 \to K^+\pi^-$ and $B^0 \to \pi^+\pi^-$, since these two decay modes feed across into each other. The feed-across fractions are constrained according to the identification efficiencies and fake rates of kaons and pions. A simultaneous fit is also used for the $B^+ \to K^+\pi^0$ and $B^+ \to \pi^+\pi^0$ decay modes.

When likelihood fits are performed, the yields are allowed to float independently for each l (set I or set II) and k bin (low or high r region). The $M_{\rm bc}$ and ΔE projections of the fits are shown in Fig. 1, while Table I summarizes the fit results for each mode. The branching fraction of each mode is calculated by dividing the total signal yield by the number of $B\overline{B}$ pairs and by the average reconstruction efficiency. The calculation of this average efficiency takes into account the differences between various l and k bins, and sub-decay branching fractions.

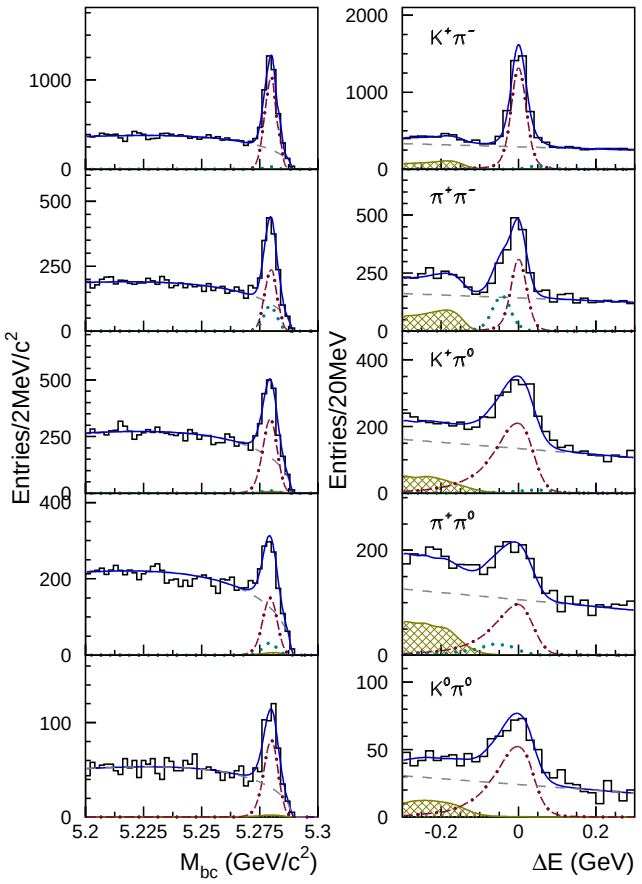

FIG. 1: $M_{\rm bc}$ (left) and ΔE (right) distributions for $B^0 \to K^+\pi^-$, $B^0 \to \pi^+\pi^-$, $B^+ \to K^+\pi^0$, $B^+ \to \pi^+\pi^0$ and $B^0 \to K^0\pi^0$ candidates. The histograms show the data, while the curves represent the various components from the fit: signal (dot-dashed), continuum (dashed), charmless B decays (hatched), background from mis-identification (dotted), and sum of all components (solid). The $M_{\rm bc}$ and ΔE projections of the fits are for events that have $|\Delta E| < 0.06$ GeV (left) and 5.271 GeV/c^2 $< M_{\rm bc} <$ 5.289 GeV/c^2 (right). (A looser requirement, -0.14 GeV $< \Delta E < 0.06$ GeV, is used for the modes with a π^0 meson in the final state.)

The fitting systematic errors are due to signal PDF modeling, charmless B background modeling, and feed-across constraints. The first and last of these errors are estimated from the fit deviations after varying each parameter of the signal PDFs or the yields of the feed-across backgrounds by one standard deviation. The effects due to fake-rate uncertainties are also included in the systematic error of the feed-across backgrounds. The systematic error due to the charmless B background modeling is evaluated by requiring that $\Delta E > -0.12$ GeV, since the ΔE values of the charmless B events are typically smaller than -0.12 GeV. The above deviations in the signal yield are added in quadrature to obtain the overall systematic error due to fitting.

The MC-data efficiency difference due to the requirement on the likelihood ratio $\mathcal{R}$ is investigated with $B^+ \to \overline{D}^0\pi^+$ samples. The systematic error due to the charged-track reconstruction efficiency is estimated to be 1% per track using partially reconstructed D^* events. The systematic error due to the $\mathcal{R}(K/\pi)$ selection is 1.3% for pions and 1.5% for kaons, respectively. The K^0_S reconstruction and the systematic error is verified by comparing the ratio of $D^+ \to K^0_S\pi^+$ and $D^+ \to K^-\pi^+\pi^+$ yields with the MC expectations. The π^0 reconstruction efficiency and the systematic error is verified by comparing the ratio of $\overline{D}^0 \to K^+\pi^-$ and $\overline{D}^0 \to K^+\pi^-\pi^0$ yields with the MC expectations. Possible systematic uncertainties due to the description of final-state radiation have been studied by comparing the latest theoretical calculations with the PHOTOS MC [21]. These uncertainties were found to be negligible and thus no systematic error is assigned due to PHOTOS. The systematic error due to the uncertainty of the total number of $B\overline{B}$ pairs is 1.3% and the error due to signal MC statistics is between 0.4% and 0.7%. The final systematic uncertainty is obtained by quadratically summing all the contributions, as shown in Table II.

The ratios of partial widths can be used to extract the angle ϕ_3 and to search for new physics [5, 7, 8]. These ratios (listed in Table III) are obtained from the five measurements in Table I and the new measurement of $\mathcal{B}(B^+ \to K^0\pi^+) = (22.8^{+0.8}_{-0.7} \pm 1.3) \times 10^{-6}$ described in Ref. [9]. The ratio of charged to neutral B meson lifetime, $\tau_{B^+}/\tau_{B^0} = 1.076 \pm 0.008$ [4], is used to convert the branching-fraction ratios into the ratios of partial widths. The total errors are reduced because of the cancellation

TABLE I: Extracted signal yields, product of efficiencies and sub-decay branching ratios ($\mathcal{B}_s$), and calculated branching fractions for individual modes. The branching fraction errors are statistical and systematic, respectively.

Mode	Yield	Eff.$\times\mathcal{B}_s$(%)	$\mathcal{B}(10^{-6})$
$K^+\pi^-$	3585^{+69}_{-68}	40.16	$19.9 \pm 0.4 \pm 0.8$
$\pi^+\pi^-$	872^{+41}_{-40}	37.98	$5.1 \pm 0.2 \pm 0.2$
$K^+\pi^0$	1493^{+57}_{-55}	26.86	$12.4 \pm 0.5 \pm 0.6$
$\pi^+\pi^0$	693^{+46}_{-43}	23.63	$6.5 \pm 0.4\ ^{+0.4}_{-0.5}$
$K^0\pi^0$	379^{+28}_{-27}	9.17	$9.2 \pm 0.7\ ^{+0.6}_{-0.7}$

TABLE II: Summary of systematic errors, given in percent.

	$K^+\pi^-$	$\pi^+\pi^-$	$K^+\pi^0$	$\pi^+\pi^0$	$K^0\pi^0$
Signal PDF	±0.2	±0.3	±0.4	±0.5	$^{+0.3}_{-0.4}$
Charmless B background	$^{+0.0}_{-0.2}$	$^{+0.6}_{-0.0}$	$^{+0.0}_{-0.9}$	$^{+0.0}_{-5.0}$	$^{+0.0}_{-3.0}$
Feed-across background	$^{+0.4}_{-0.3}$	$^{+2.2}_{-2.1}$	$^{+0.7}_{-0.6}$	$^{+2.5}_{-2.4}$	0.0
$\mathcal{R}$ requirement	±1.0	±1.0	±1.3	±1.4	±1.5
Tracking	±2.0	±2.0	±1.0	±1.0	0.0
$\mathcal{R}(K/\pi)$ requirement	±2.9	±2.8	±1.5	±1.3	0.0
K^0_S reconstruction	0.0	0.0	0.0	0.0	±4.9
π^0 reconstruction	0.0	0.0	±4.0	±4.0	±4.0
# of $B\overline{B}$	±1.3	±1.3	±1.3	±1.3	±1.3
Signal MC statistics	±0.6	±0.4	±0.4	±0.5	±0.7
Total	±4.0	$^{+4.5}_{-4.4}$	$^{+4.8}_{-4.9}$	$^{+5.4}_{-7.3}$	$^{+6.7}_{-7.3}$

TABLE III: Partial width ratios of $B \to K\pi$ and $\pi\pi$ decays. The errors are quoted in the same manner as in Table I.

Modes	Ratio
$2\Gamma(K^+\pi^0)/\Gamma(K^0\pi^+)$	$1.08 \pm 0.06 \pm 0.08$
$\Gamma(K^+\pi^-)/2\Gamma(K^0\pi^0)$	$1.08 \pm 0.08\ ^{+0.09}_{-0.08}$
$\Gamma(K^+\pi^-)/\Gamma(K^0\pi^+)$	$0.94 \pm 0.04 \pm 0.05$
$\Gamma(\pi^+\pi^-)/\Gamma(K^+\pi^-)$	$0.26 \pm 0.01 \pm 0.01$
$\Gamma(\pi^+\pi^-)/2\Gamma(\pi^+\pi^0)$	$0.42 \pm 0.03\ ^{+0.03}_{-0.02}$
$\Gamma(\pi^+\pi^0)/\Gamma(K^0\pi^0)$	$0.66 \pm 0.07 \pm 0.05$
$2\Gamma(\pi^+\pi^0)/\Gamma(K^0\pi^+)$	$0.57 \pm 0.04\ ^{+0.04}_{-0.05}$

of some common systematic errors. With a factor of five times more data than that used for our previous published results [1], the statistical errors on the branching fractions for all decay modes are reduced by more than a factor of 2.3. The central value of the $K^0\pi^0$ branching fraction has decreased from 11.7×10^{-6} to 9.2×10^{-6} and the $K^+\pi^-$ branching fraction has increased from 18.5×10^{-6} to 19.9×10^{-6}, resulting in a change in R_n from 0.79 ± 0.18 to 1.08 ± 0.12. The obtained value of $R_c = 1.08 \pm 0.09$ is similar to the previous Belle measurement (1.09 ± 0.19) but is more precise. The errors for R_n and R_c shown here are the sum in quadrature of the statistical and systematic errors. These two ratios are now consistent with SM expectations [5, 6, 7, 8].

In conclusion, we have measured the branching fractions for $B \to K\pi$ and $B \to \pi\pi$ decays with 449 million $B\overline{B}$ pairs collected at the $\Upsilon(4S)$ resonance with the Belle detector. We confirm the expected hierarchy of branching fractions : $\mathcal{B}(K^0\pi^+) \geq \mathcal{B}(K^+\pi^-) > \mathcal{B}(K^+\pi^0) \geq \mathcal{B}(K^0\pi^0) > \mathcal{B}(\pi^+\pi^0) \geq \mathcal{B}(\pi^+\pi^-)$ and find no significant deviation from SM expectations in the ratios of partial widths. We also find that the ratios R_n and R_c are both in good agreement with SM expectations, in contrast to early measurements [1, 2, 3].

We thank the KEKB group for excellent operation of the accelerator, the KEK cryogenics group for efficient solenoid operations, and the KEK computer group and the NII for valuable computing and Super-SINET network support. We acknowledge support from MEXT and JSPS (Japan); ARC and DEST (Australia); NSFC and KIP of CAS (China); DST (India); MOEHRD, KOSEF and KRF (Korea); KBN (Poland); MIST (Russia); ARRS (Slovenia); SNSF (Switzerland); NSC and MOE (Taiwan); and DOE (USA).

[1] Y. Chao *et al.* (Belle Collaboration), Phys. Rev. D **69**, 111102 (2004).
[2] B. Aubert *et al.* (BaBar Collaboration), Phys. Rev. D **71**, 111102 (2005); Phys. Rev. Lett. **94**, 181802 (2005); Phys. Rev. Lett. **97**, 171805 (2006); Phys. Rev. D **75**, 012008 (2007).
[3] A. Bornheim *et al.* (CLEO Collaboration), Phys. Rev. D **68**, 052002 (2003).
[4] The average results in Winter 2006 by the HFAG group.
[5] A. J. Buras, R. Fleischer, S. Recksiegel and F. Schwab, Eur. Phys. J. C **45**, 701 (2006).
[6] H.-n. Li, S. Mishima and A. I. Sanda, Phys. Rev. D **72**, 114005 (2005).
[7] T. Yoshikawa, Phys. Rev. D **68**, 054023 (2003); S. Mishima, T. Yoshikawa, Phys. Rev. D **70**, 094024 (2004).
[8] M. Gronau and J. L. Rosner, Phys. Lett. B **572**, 43 (2003).
[9] K. Abe *et al.* (the Belle Collaboration), hep-ex/0608049, submitted to the Phys. Rev. Lett..
[10] Y. Chao *et al.* (Belle Collaboration), Phys. Rev. Lett. **94**, 181803 (2005).
[11] S. Kurokawa and E. Kikutani, Nucl. Instr. Meth. A **499**, 1 (2003), and other papers included in this volume.
[12] A. Abashian *et al.* (Belle Collaboration), Nucl. Instr. Meth. A **479**, 117 (2002).
[13] Z. Natkaniec *et al.* (Belle SVD2 Group), Nucl. Instr. Meth. A **560**, 1 (2006).
[14] W.-M. Yao *et al.* (Particle Data Group), J. Phys. G **33**, 1 (2006).
[15] The K^0_S selection is described in K. -F. Chen *et al.* (Belle Collaboration), Phys. Rev. D **72**, 012004 (2005).
[16] G. C. Fox and S. Wolfram, Phys. Rev. Lett. **41** 1581 (1978). The modified moments used in this paper are described in, S. H. Lee *et al.* (Belle Collaboration), Phys. Rev. Lett. **91**, 261801 (2003).
[17] R. Brun *et al.*, GEANT 3.21, CERN Report No. DD/EE/84-1 (1987).

[18] H. Kakuno *et al.*, Nucl. Instr. and Meth. A **533**, 516 (2004).

[19] E. Barberio and Z. Was, Comput. Phys. Commun. **79**, 291 (1994); P. Golonka and Z. Was, hep-ph/0506026. We use PHOTOS version 2.13 allowing the emission of up to two photons, with an energy cut-off at 1% of the energy available for photon emission (i.e. approximately 26 MeV for the first emitted photon). PHOTOS also takes into account interference between charged final-state particles.

[20] H. Albrecht *et al.* (ARGUS Collaboration), Phys. Lett. B **241**, 278 (1990).

[21] G. Nanava and Z. Was, hep-ph/0607019.